

RESEARCH

Open Access



Dapagliflozin attenuates metabolic dysfunction-associated steatotic liver disease by inhibiting lipid accumulation, inflammation and liver fibrosis

Xingyu Fan^{1,2†}, Yueyue Wang^{1,2†}, Yue Wang^{1,2†}, Hao Duan^{1,2}, Yijun Du^{1,2}, Tianrong Pan^{1,2*} and Xing Zhong^{1,2*}

Abstract

Background Metabolic dysfunction-associated steatotic liver disease (MASLD) has emerged as a globally prevalent liver disease, closely linked to the rising incidence of obesity, diabetes, and metabolic syndrome. Dapagliflozin (DaPa), a sodium-glucose cotransporter-2 inhibitor, is primarily prescribed for diabetes management. It has shown potential efficacy in managing MASLD in clinical settings. However, the molecular mechanisms underlying the effects of DaPa on MASLD remain poorly understood. Hence, we aimed to investigate the role of and mechanisms underlying DaPa in MASLD.

Methods Male diet-induced obese (DIO) C57BL/6J mice were injected with streptozotocin (STZ), followed by a high-fat diet regimen to stimulate metabolic dysfunction. Subsequently, they received DaPa via gavage for 5 weeks. Hepatic lipid accumulation, pathological alterations, inflammatory markers, and liver fibrosis were assessed.

Results DaPa administration reduced liver fat accumulation in DIO mice. Additionally, it decreased oxidative stress and lipid peroxide levels, which was attributed to the upregulation of glutathione and the downregulation of malondialdehyde and reactive oxygen species levels. Notably, DaPa downregulated the inflammatory response and reduced liver fibrosis.

Conclusions DaPa protects against MASLD by inhibiting lipid accumulation, inflammation, oxidative stress, and liver fibrosis.

Keywords Dapagliflozin, Metabolic dysfunction-associated steatotic liver disease, Lipid accumulation, Inflammation, Oxidative stress, Fibrosis

[†]Xingyu Fan, Yueyue Wang and Yue Wang contributed equally to this work.

*Correspondence:
Tianrong Pan
PanTR1968@163.com
Xing Zhong
zhongxing761@163.com

¹Department of Endocrinology, The Second Affiliated Hospital of Anhui Medical University, No. 678 Furong Road, Jingkai District, Hefei, Anhui Province 230601, China

²Research Center for Translational Medicine, The Second Affiliated Hospital of Anhui Medical University, No. 678 Furong Road, Jingkai District, Hefei, Anhui Province 230601, China



Introduction

Metabolic dysfunction-associated steatotic liver disease (MASLD) is a leading cause of chronic liver diseases globally, affecting approximately 25% of adults [1]. MASLD is characterized by excessive fat accumulation in the liver in the absence of substantial alcohol consumption [2]. It spans a spectrum that comprises simple steatosis, metabolic dysfunction-associated steatohepatitis, fibrosis, cirrhosis, and even hepatocellular carcinoma [3]. MASLD pathophysiology consists of interrelated processes, including hepatic fat accumulation, oxidative stress, inflammation, and fibrosis [4], all of which drive disease progression and liver damage. Despite its increasing prevalence and associated health risks, pharmacological treatments for MASLD remain limited. The management strategies primarily emphasize lifestyle modifications and managing metabolic comorbidities [5]. Thus, there is a growing interest in identifying therapeutic agents targeting the mechanisms underlying MASLD.

Risk factors for MASLD consists of obesity, type 2 diabetes mellitus (T2DM), hypertension, and dyslipidemia. Notably, the prevalence of MASLD is significantly high among individuals with T2DM, affecting between one-third and two-thirds of this population [6–8]. Metabolic dysfunction and chronic suboptimal glucose regulation induce impaired insulin signaling pathways and contribute to MASLD; therefore, hypoglycemic agents have been investigated for their benefits in managing MASLD [9]. Combining the hypoglycemic agent Dapagliflozin (DaPa) with metformin or exenatide enhances MASLD treatment outcomes in patients with T2DM [10, 11]. DaPa, a sodium-glucose cotransporter-2 (SGLT2) inhibitor, lowers blood glucose levels by inhibiting glucose reabsorption in the proximal convoluted tubules of the kidneys. Additionally, it facilitates urinary glucose excretion [12].

Recent studies have demonstrated the therapeutic potential of DaPa in patients with T2DM complicated with MASLD [13–15]. Moreover, randomized controlled trials have confirmed that SGLT-2 inhibitors can reduce liver enzymes levels, intrahepatic fat content and liver fibrosis markers [16, 17]. Parallel to clinical findings, preclinical investigations have extensively explored the pharmacological effects of SGLT2 inhibitors on hepatic steatosis and lipid metabolism using high-fat diet (HFD)-induced obesity models. Notably, Luo et al. [18] provided mechanistic insights by demonstrating that DaPa ameliorates hepatic steatosis in HFD-fed mice through modulation of the AMPK/mTOR signaling pathway. Complementing these findings, Hana et al. [19] reported that DaPa administration significantly reduced adiposity and improved hepatic steatosis independent of body weight changes. Furthermore, recent mechanistic studies by Xiang et al. [20] revealed that DaPa promotes white adipose tissue browning and enhances lipid utilization,

providing additional evidence for its therapeutic efficacy in obesity-associated liver pathologies. Despite these significant advances, the precise molecular mechanisms underlying DaPa's beneficial effects on MASLD pathogenesis remain to be fully elucidated, warranting further investigation.

In this study, we used diet-induced obese (DIO) mice with MASLD to evaluate the action of DaPa on the liver. We focus on the potential mechanisms through which DaPa exerts these effects, particularly in terms of oxidative stress, lipid metabolism, and inflammatory responses. Our findings may provide further insights into the therapeutic potential of DaPa for managing MASLD and related metabolic disorders.

Materials and methods

Animal treatment

Male C57BL/6J mice at five weeks of age were obtained from a commercial supplier (Hangzhou Ziyuan Laboratory Animal Technology Co., Ltd., China). The mice were maintained in a controlled environment with ad libitum access to food and water. Following a one-week acclimatization period, the mice were allocated into two groups: a normal diet group (CON, $n=6$) and a high-fat diet (HFD) group. The HFD, formulated as a rodent diet with a fat content of 60 Kcal% (D12492), was employed to induce obesity and glucose intolerance. After 4 weeks, the HFD group mice were transferred to a biohazard facility for streptozotocin (STZ) administration. STZ was prepared as a 1% solution in sodium citrate buffer (pH 4.5) and administered intraperitoneally at a dose of 100 mg/kg body weight to induce partial pancreatic islet cell destruction, a critical step in modeling metabolic dysfunction. Prior to STZ injection, mice were fasted for 12 h, and their body weights were recorded to determine the appropriate dose. Post-STZ administration, the HFD group mice were further randomized into two groups: diet-induced obesity (DIO, $n=6$) and DIO treated with dapagliflozin (DIO + DaPa, $n=6$). After 12 weeks, the DIO + DaPa group received DaPa (1 mg/kg) via oral gavage once daily for 5 weeks. Concurrently, the CON and DIO groups were administered a vehicle (0.5% carboxymethylcellulose). Both the DIO and DIO + DaPa groups continued on the high-fat diet from 6 weeks of age until the conclusion of the experiment. At the experimental endpoint, mice were anesthetized via intraperitoneal injection of pentobarbital, followed by cervical dislocation for euthanasia. Liver tissues were promptly excised, weighed, and cryopreserved at $-80\text{ }^{\circ}\text{C}$ for further biochemical investigations. Blood glucose levels were monitored weekly using a blood glucose meter (OneTouch Verio Flex) through tail vein blood sampling. The experimental protocol was performed in strict accordance with institutional ethical standards, adhering to

both the ARRIVE Guidelines and institutional animal care protocols, following approval by the Animal Experiment and Ethics Committee of the Second Affiliated Hospital, Anhui Medical University.

Serum biochemical analysis

Serum levels of total cholesterol (TC), triglycerides (TG), low-density lipoprotein cholesterol (LDL-C), and high-density lipoprotein cholesterol (HDL-C) were quantified using commercially available assay kits (Nanjing Jiancheng Institute of Bioengineering, Nanjing, China) according to the manufacturer's instructions. Briefly, lipid parameters in serum samples were analyzed using a multi-mode microplate reader (Thermo, Varioskan Lux, USA). Absorbance readings were taken at 500 nm for TC and TG, and at 600 nm for LDL-C and HDL-C.

Lipid peroxidation products

Liver tissue homogenization and centrifugation were performed to obtain a homogenate, from which the supernatant was harvested. The BCA assay was utilized to measure protein levels. Following this, measurements of glutathione (GSH) and malondialdehyde (MDA) levels were conducted independently following the kit instructions (Nanjing Jiancheng Bioengineering Institute). GSH and MDA levels were quantified at 405 and 532 nm, respectively, using a multifunctional microplate reader (Thermo, Varioskan Lux).

Quantification of intracellular reactive oxygen species (ROS) in liver tissue

The measurement of intracellular ROS was performed utilizing 2',7'-dichlorofluorescein diacetate (DCFH-DA) as a fluorescence-based detection reagent (Elabscience, E-BC-K138-F). Briefly, a single-cell suspension of liver tissue was prepared via mechanical dissociation. The cell suspension was incubated with 10 μ M DCFH-DA at 37 °C for 45 min under light-protected conditions. Following incubation, the cells were centrifuged at 1000 \times g for 10 min, washed three times with serum-free culture medium, and resuspended in the same medium. Fluorescence intensity measurements were conducted using a microplate reader with respective excitation and emission wavelengths configured at 500 nm and 525 nm.

Histopathological and hepatic lipid analysis

First, liver sections were meticulously harvested, fixed in 4% paraformaldehyde, and embedded in paraffin. Second, the sections were subjected to hematoxylin and eosin (H&E) staining, Masson's trichrome staining, and Sirius Red staining at room temperature. Third, frozen liver tissues were stained with Oil-Red O utilizing a commercially available kit (Servicebio, Wuhan, China), adhering strictly to the manufacturer's instructions. Finally, the

stained sections underwent histopathological evaluation under an Olympus BX41 microscope.

In order to quantify lipid accumulation in liver tissue, TG and TC content were measured in liver tissue. Approximately 20 mg of liver tissue was weighed and ground with 180 μ L of absolute ethanol to prepare tissue homogenate, centrifuged, and the supernatant was collected for further analysis. The levels of TC and TG in liver tissue were measured using the same assay kit (Nanjing Jiancheng Institute of Bioengineering, Nanjing, China) and method as serum samples. Measure the absorbance of TC and TG at 500 nm using a microplate reader.

Immunohistochemistry

Protein localization analysis was performed on 5- μ m hepatic tissue sections prepared from formalin-fixed, paraffin-embedded samples following standardized immunohistochemical procedures [21]. Tissue sections underwent sequential processing, including dewaxing in xylene, rehydration through graded alcohols, and endogenous peroxidase blockade using 3% hydrogen peroxide. Heat-mediated antigen retrieval was achieved through citrate buffer immersion (10 mM, pH 6.0), followed by blocking with 10% goat serum at physiological temperature (37 °C) for 60 min. Primary antibody incubation was carried out at 4 °C for 12–16 h using specific markers: F4/80 (Affinity, DF2789; 1:300 dilution) for macrophage identification, MPO (Proteintech, 22225-1-AP; 1:400) for neutrophil detection, collagen I (Servicebio, GB11022; 1:200), α -SMA (Servicebio, GB111364; 1:300), and fibronectin (Servicebio, GB114491; 1:1500) for extracellular matrix components. Chromogenic detection was performed using a HRP-DAB detection kit (ZSGBBIO, China), with hematoxylin counterstaining for nuclear visualization. Following ethanol dehydration and xylene clearing, mounted sections were examined using an Olympus BX41 light microscope for image acquisition.

Quantitative real-time polymerase chain reaction

Total RNA was extracted from liver tissues using Trizol reagent (Thermo Fisher Scientific, Waltham, USA). Complementary DNA (cDNA) was synthesized using the HyperScript TM III 1st Strand cDNA Synthesis Kit (NovaBio, Shanghai, China). Quantitative real-time polymerase chain reaction (qRT-PCR) was conducted using the S6 Universal SYBR qPCR mix (NovaBio, Shanghai, China) and the ABI 7900 PCR system (ABI, USA). Relative gene expression was determined using the 2^{- $\Delta\Delta$ Ct} method, with glyceraldehyde-3-phosphate dehydrogenase serving as the internal control. Customized primers were synthesized by Genscript, with the primer sequences described in Supplementary Table 1.

DNA fragmentation analysis using TUNEL staining

During genomic DNA breaks, the exposed 3'-OH ends can undergo catalysis by terminal deoxynucleotidyl transferase to incorporate fluorescein- and biotin-labeled deoxyuridine triphosphate (dUTP), facilitating cell apoptosis detection through fluorescence microscopy or chemical colorimetric methods. First, tissue sections were deparaffinized and rehydrated using the terminal deoxynucleotidyl transferase dUTP nick-end labeling (TUNEL) kit (Elabscience, cat number: E-CK-A320) per the manufacturer's instructions. Second, the sections were permeabilized with Proteinase K (1×) for 20 min and incubated with TUNEL reagent for 1 h at 37 °C. Third, after rinsing with phosphate-buffered saline, the sections were sealed with coverslips. Finally, fluorescein isothiocyanate labeled TUNEL-positive cells were visualized using fluorescence microscopy, while apoptosis was observed under a Leica DMI3000B microscope. TUNEL-positive cells were quantified using ImageJ software.

Data analysis and statistical methods

Data are presented as mean ± SEM. All statistical computations were performed using GraphPad Prism 8.0. For comparison of two experimental groups, unpaired two-tailed Student's t-test was applied. Multiple group comparisons were analyzed by one-way ANOVA with Tukey's post hoc test for intergroup comparisons. The threshold for statistical significance was established at $P < 0.05$.

Results

DaPa alleviates liver injury in DIO mice

STZ-treated DIO mice have been established as a MASLD mouse model. (Fig. 1A). The liver-to-body weight ratio and blood glucose levels were increased in DIO mice. In contrast, DaPa-treatment reversed these trends (Fig. 1B). Hepatic steatosis was successfully induced, as demonstrated by significant elevations in TC, HDL-C, and LDL-C levels, whereas TG levels were maintained at baseline values. What's more, DaPa treatment reduced blood lipid indicators, including TC and LDL-C (Fig. 1C). Histopathological examination via H&E staining indicated notable improvement in hepatocyte ballooning in DIO mice after DaPa treatment (Fig. 1D). Collectively, DaPa treatment significantly decreased blood glucose levels, reduced serum cholesterol, and attenuated liver injury in DIO mice.

DaPa inhibited inflammatory response in mice with DIO-induced liver injury

Inflammation is central to MASLD pathogenesis. Hence, we conducted qRT-PCR to assess the expression of inflammatory factors and chemokines. Significant differences were observed in the mRNA levels of *IL-6*, *TNF-α*, *Ptgs2*, *CCL2*, *CXCL1*, *CXCL1*, *CXCL2* between CON

and DIO groups, with these levels decreasing after DaPa treatment (Fig. 2A and B). These findings underscore the capacity of DaPa to ameliorate liver inflammation in DIO mice. Immunohistochemistry analysis suggested elevated levels of the neutrophil marker MPO and macrophage marker F4/80 in the DIO group, compared with the CON group. Notably, DaPa treatment markedly reduced MPO and F4/80 levels in DIO mice (Fig. 2C and D), highlighting its anti-inflammatory potential in DIO-induced liver injury.

DaPa suppresses oxidative stress in DIO mice

Compared with the CON group, Oil Red O staining analysis demonstrated enhanced lipid droplet accumulation in the DIO group. However, after 5 weeks of DaPa, hepatocyte steatosis was reduced (Fig. 3A). Hepatic lipid accumulation is a key indicator of hepatic steatosis. To evaluate the impact of DaPa on liver lipids, we measured hepatic TC and TG levels. Compared to the control group, DIO mice exhibited a significant increase in hepatic TC, which was markedly reduced following DaPa treatment. In contrast, although a downward trend in hepatic TG levels was observed after DaPa administration, the change did not reach statistical significance (Fig. 3B). Lipid peroxidation was evaluated by measuring the antioxidant capacity. Glutathione (GSH) content was reduced in the DIO group than in the CON group, despite remaining unaffected in the DIO+DaPa group. Conversely, malondialdehyde (MDA) levels, which were significantly increased in the DIO group, were markedly reduced after DaPa treatment (Fig. 3C). Moreover, the expression of reactive oxygen species (ROS) was higher in both DIO and DIO+DaPa groups (Fig. 3D). The C/EBP-homologous protein (CHOP) and activating transcription factor 4 (ATF4) interact in the endoplasmic reticulum stress response to promote cell death, while X-box binding protein 1 (XBP1) regulates lipid metabolism and unfolded protein responses, which together promote the pathogenesis of MASLD. qRT-PCR analysis showed that DaPa treatment upregulated factors involved in oxidative stress, including activation *ATF4*, *Chop*, and *XBP1* (Fig. 3E).

DaPa improves liver fibrosis

Histopathological evaluation through Sirius Red and Masson staining revealed significant extracellular matrix deposition in diet-induced obese (DIO) mice (Fig. 4A and B). Collagen I and fibronectin contribute to liver fibrosis by promoting the accumulation of extracellular matrix proteins, thus exacerbating MASLD progression. Immunohistochemical staining confirmed elevated levels of α-SMA, collagen I, and fibronectin in the DIO group (Fig. 4C-E). Collectively, these findings indicate liver

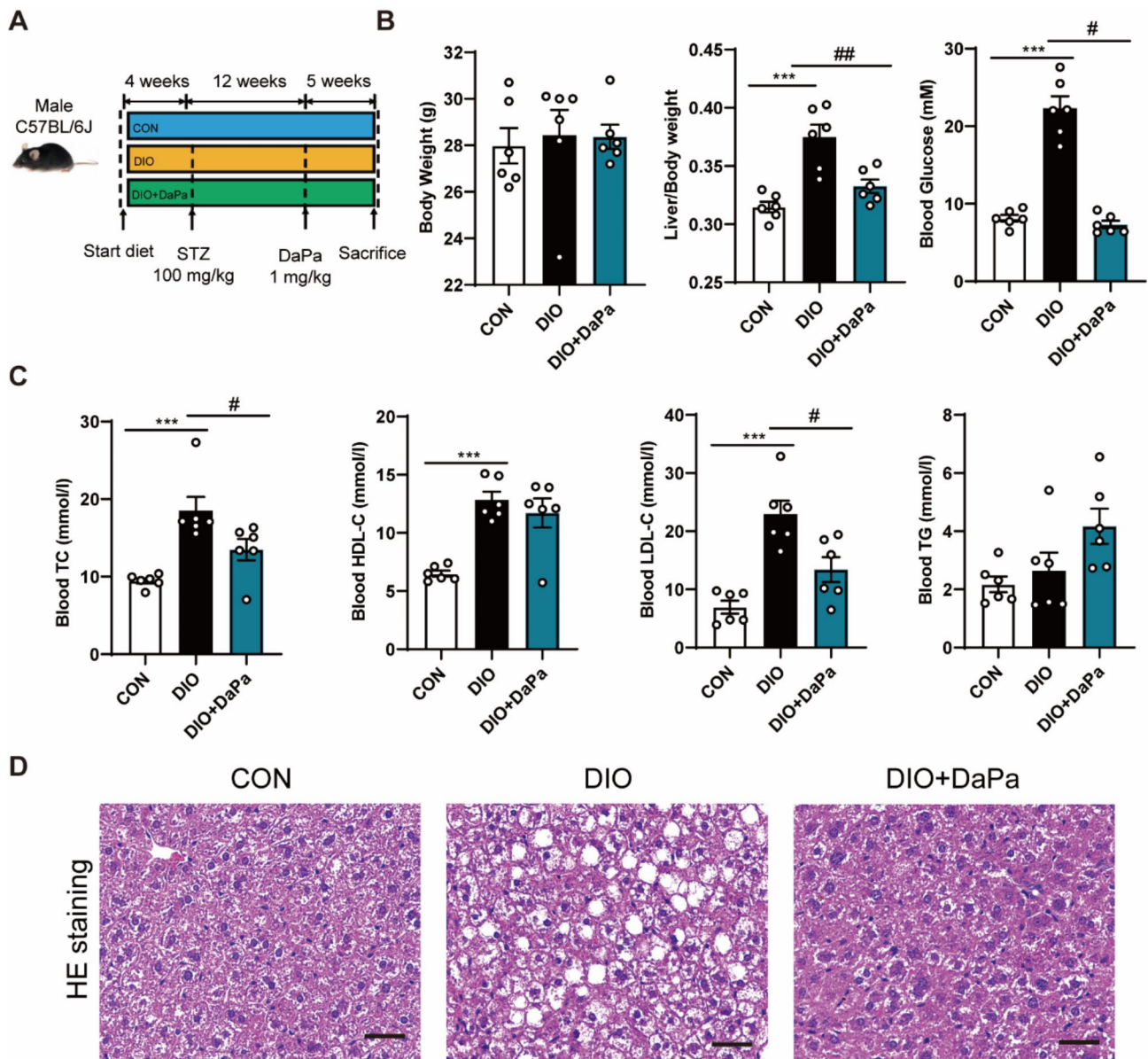


Fig. 1 DaPa alleviates liver injury in DIO mice. **(A)** Schematic diagram of the experimental design for the mouse model. **(B)** Impact of DaPa on the body weight, liver-to-body weight ratio, and blood glucose levels in CON, DIO, and DIO+DaPa mice. **(C)** Serum levels of TC, HDL-C, LDL-C, and TG across different groups. **(D)** Histopathological alterations are assessed via H&E staining. (scale bar, 100 μ m). Data are presented as mean \pm SD ($n=6$). ** $p < 0.01$, *** $p < 0.001$, *comparison between the CON and DIO groups; # $p < 0.05$, #comparison between the DaPa-treated and DIO groups

injury accompanied by fibrosis in DIO mice and DaPa treatment ameliorated this fibrotic condition.

Effects of DaPa on hepatocyte apoptosis

To explore the mechanism by which DaPa mitigates liver injury, we examined hepatocyte apoptosis levels using TUNEL staining. TUNEL-positive cells were significantly increased in the DIO group (Fig. 5). Concurrently, pharmacological intervention with DaPa markedly decreased the population of TUNEL-positive hepatocytes, demonstrating its therapeutic potential in suppressing apoptosis in DIO mice with liver injury. (Fig. 5A and B).

Discussion

MASLD represents a critical metabolic disorder with increasing prevalence [22], particularly among individuals with obesity and T2DM [23]. Despite its significant health implications, effective pharmacological treatments for MASLD remain limited. In this study, we investigated the effects of DaPa, an SGLT2 inhibitor, on MASLD in DIO mice, focusing on its impact on lipid accumulation, inflammation, oxidative stress, and liver fibrosis.

Our findings demonstrate that DaPa attenuates hepatic lipid accumulation, as evidenced by reduced liver weight, decreased lipid droplet deposition, and

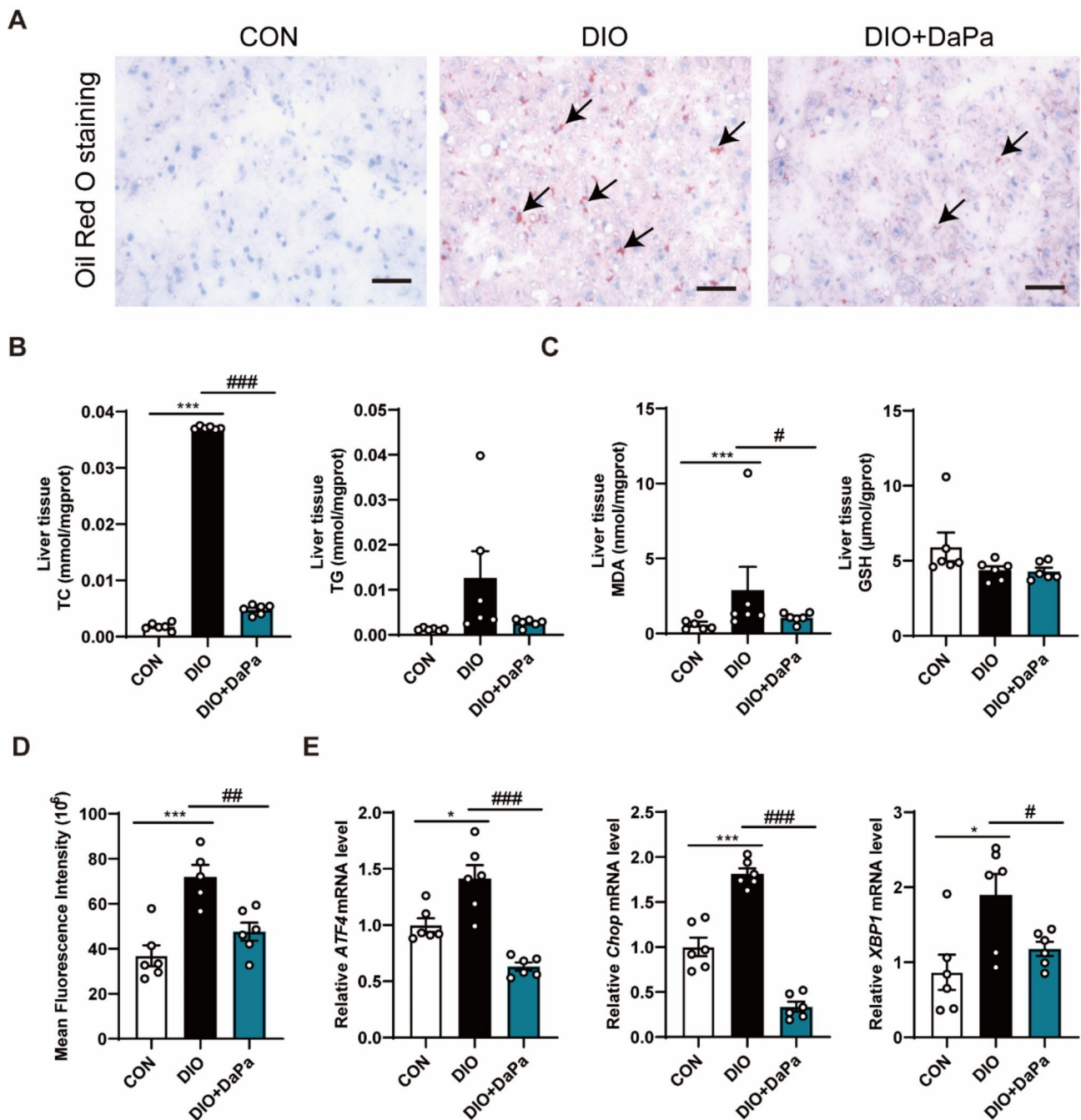


Fig. 3 DaPa suppresses oxidative stress in DIO mice. **(A)** Representative liver images stained with Oil Red O. (scale bar, 100 μm). **(B)** TG and TC levels in the CON, DIO, and DIO+DaPa groups. **(C)** MDA and GSH levels in liver tissues. **(D)** Histogram of relative fluorescence intensity of ROS in liver tissues. **(E)** mRNA levels of ATF4, CHOP, and XBP1 in CON, DIO, and DIO+DaPa groups. Data are presented as mean ± SD ($n=6$). * $p < 0.05$, ** $p < 0.01$, and *** $p < 0.001$, *comparison between the CON and DIO groups; # $p < 0.05$, ## $p < 0.01$, ### $p < 0.001$, #comparison between the DaPa-treated and DIO groups

improved histological features of MASLD in DIO mice. These findings align with previous studies showing that SGLT2 inhibitors reduce hepatic fat content and ameliorate hepatic steatosis in both rodent models and human patients with T2DM and MASLD [18, 24]. In this study, we successfully induced hepatic steatosis in DIO mice, characterized by elevated hepatic TC and TG levels [25].

Mechanistically, the reduction in hepatic lipid accumulation is likely mediated by enhanced fatty acid oxidation and suppressed lipogenesis, as indicated by the upregulation of key lipid metabolism-related genes such as PPAR α , PGC1- α , and CPT1 α in the liver [19, 26]. These findings align with the metabolic substrate shift hypothesis, wherein SGLT2 inhibitors promote a shift

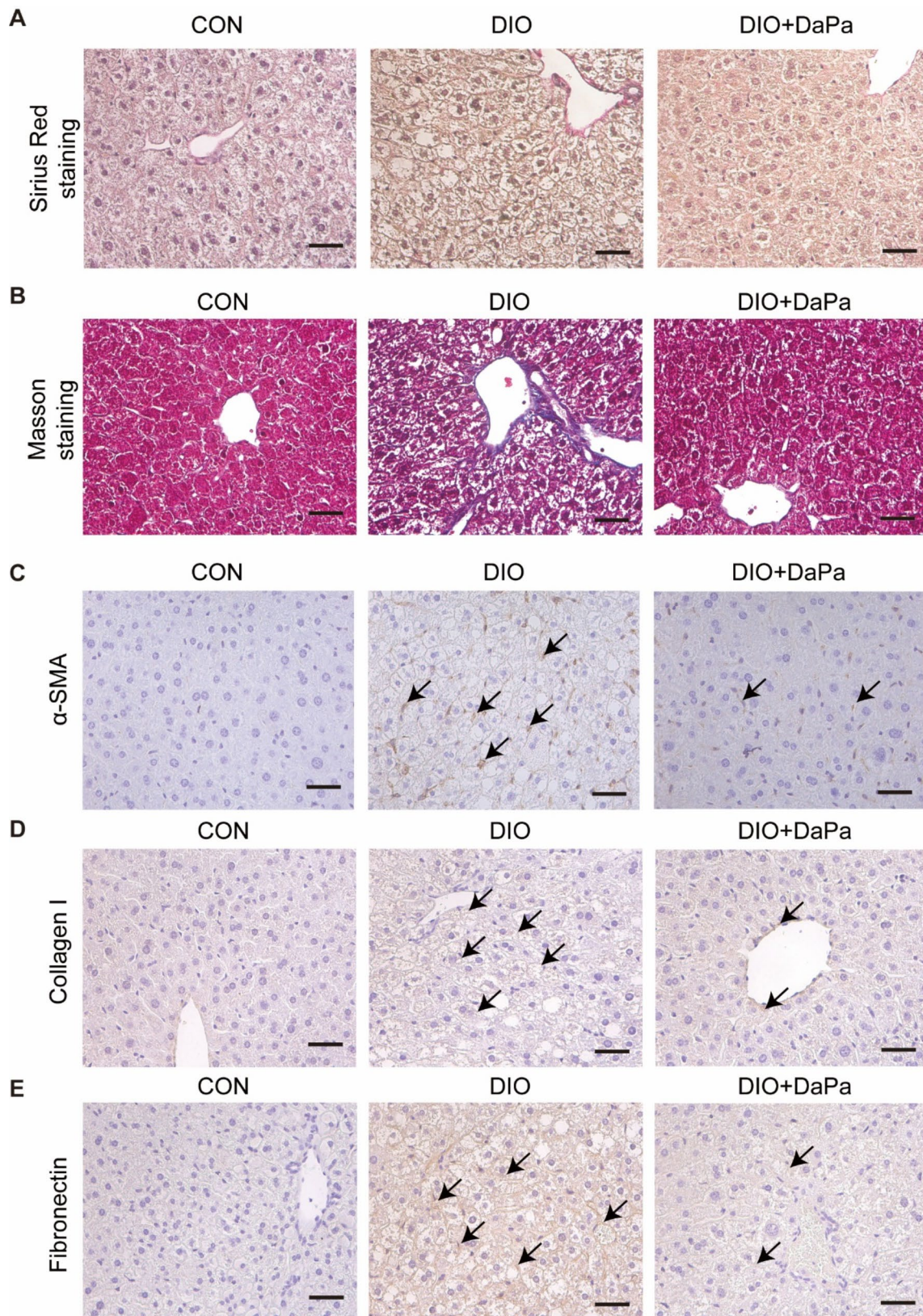


Fig. 4 DaPa improves liver fibrosis in DIO mice. **(A, B)** Sirius Red staining **(A)** and Masson's Trichrome staining **(B)** in liver tissues from CON, DIO, and DIO+DaPa groups (scale bar, 100 μ m). **(C, D, E)** Immunohistochemical staining of liver tissues for α -SMA **(C)**, collagen I **(D)**, and fibronectin **(E)** (scale bar, 100 μ m). Data are presented as mean \pm SD ($n=6$)

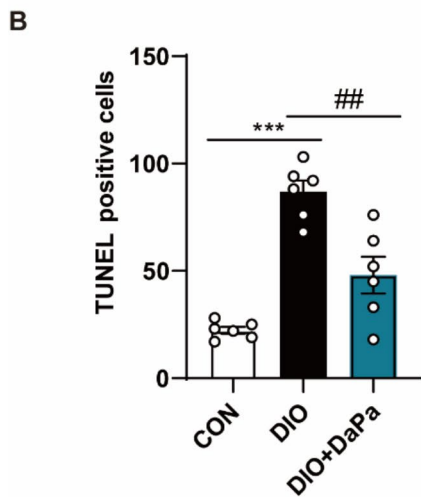
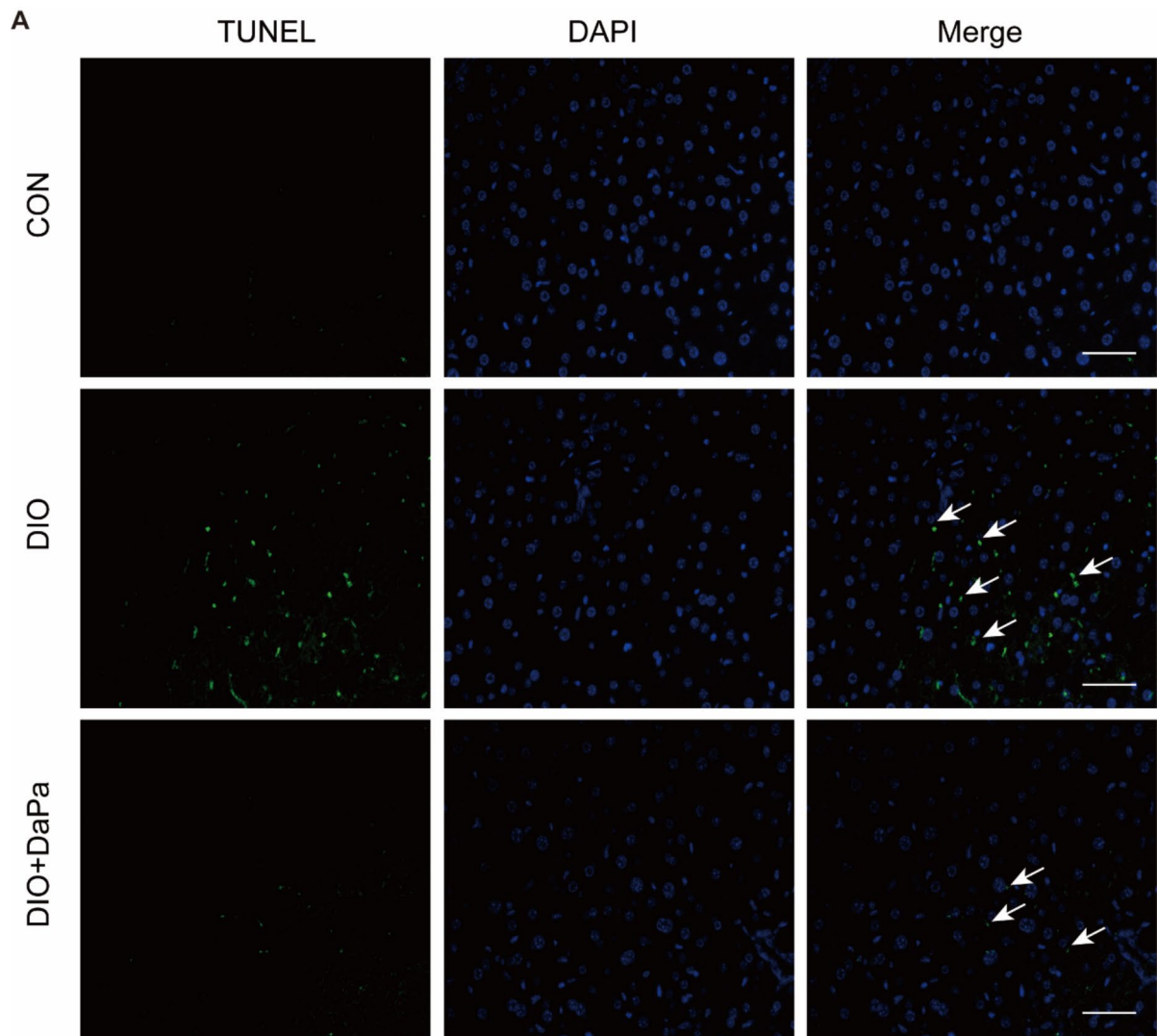


Fig. 5 Effects of DaPa on hepatocyte apoptosis. **(A)** TUNEL staining indicates hepatocyte apoptosis across the three groups. Green arrows indicate TUNEL-positive cells. Scale bars, 100 μ m. **(B)** TUNEL-positive cells in liver tissues. Data are presented as mean \pm SD ($n=6$). *** $p < 0.01$, *comparison between the CON and DIO groups; ## $p < 0.01$, #comparison between the DaPa-treated and DIO+DaPa groups

from glucose to fatty acid utilization, thereby alleviating hepatic fat accumulation [27]. Collectively, our results further support the role of DaPa in promoting lipid metabolism and attenuating hepatic steatosis through these molecular mechanisms.

Inflammation is a key driver of MASLD progression [28] and pro-inflammatory cytokines such as IL-6 and TNF- α serve as diagnostic biomarkers for MASLD [29]. Our study revealed significant upregulation of pro-inflammatory cytokines, including TNF- α , IL-6, Ptgs2, CCL2, CXCL1, and CXCL2 in DIO mice. Notably, DaPa treatment markedly reduced the expression of these inflammatory markers. Specifically, in contrast to Han et al.'s study, which reported no significant improvement in TNF- α and IL-6 levels following 4-week DaPa treatment (1 mg/kg/day) in HFD-induced obese mice [19], our intervention achieved significant reductions in these key inflammatory mediators. Furthermore, DaPa significantly decreased the expression of macrophage marker F4/80 and neutrophil marker MPO, suggesting a reduction in inflammatory cell infiltration in the liver. These findings align with previous reports demonstrating that SGLT2 inhibitors, such as empagliflozin and canagliflozin, mitigate inflammation by modulating macrophage polarization, inhibiting the NLRP3 inflammasome pathway, and reducing systemic and tissue-specific pro-inflammatory cytokine secretion [30, 31]. For instance, Zhang et al. [32] highlighted that SGLT2 inhibitors exert anti-inflammatory effects by downregulating TNF- α , IL-6, and monocyte chemoattractant proteins, thereby improving metabolic and cardiovascular outcomes in patients with T2DM. The anti-inflammatory properties of DaPa are particularly crucial, as chronic inflammation not only drives hepatocellular injury but also creates a pro-fibrogenic microenvironment, facilitating the progression from simple steatosis to steatohepatitis and fibrosis in MASLD [33].

Building upon these anti-inflammatory effects, our study further demonstrates that DaPa ameliorates oxidative stress, another key pathological process in MASLD progression [34]. The observed significant reduction in MDA levels and increase in GSH content in DaPa-treated mice indicate improved antioxidant capacity, suggesting a restoration of redox homeostasis. These findings are consistent with previous studies demonstrating that SGLT2 inhibitors reduce oxidative stress by enhancing mitochondrial function and reducing ROS production [35, 36]. Importantly, the interplay between oxidative stress and inflammation is particularly relevant in MASLD pathogenesis, as excessive ROS can activate the NLRP3 inflammasome and perpetuate inflammatory signaling cascades [37]. The reduction in oxidative stress may also contribute to the observed decrease in liver fibrosis [38], as oxidative stress is known to activate hepatic stellate

cells (HSCs) and promote extracellular matrix deposition [39]. This connection between oxidative stress and fibrogenesis provides a mechanistic basis for understanding DaPa's multi-faceted hepatoprotective effects.

Fibrosis is a critical determinant of MASLD progression, with activated HSCs playing a central role in extracellular matrix deposition. In our study, we observed that DaPa significantly reduces fibrotic areas in the liver, as evidenced by decreased collagen deposition and expression of fibrotic markers such as α -SMA, collagen I, and fibronectin. These results align with prior studies demonstrating that SGLT2 inhibitors attenuate liver fibrosis by reducing HSC activation and collagen deposition [40]. Furthermore, Shen et al. [41] reported that empagliflozin alleviates fibrosis in MASLD by suppressing the TGF β signaling pathway in HSCs. Clinical evidence indicates that SGLT2 inhibitors significantly reduce liver stiffness in patients with type 2 diabetes and MASLD, highlighting their potential to ameliorate liver fibrosis progression [42]. The anti-fibrotic effects of DaPa may be mediated by its ability to reduce oxidative stress and inflammation, both of which are key drivers of fibrogenesis in MASLD.

The development of effective pharmacological interventions for MASLD remains a significant challenge, with limited therapeutic options currently receiving regulatory approval. Notably, resmetirom, a selective thyroid hormone receptor beta (THR- β) agonist, has recently gained attention as a potential therapeutic agent, demonstrating efficacy in reducing both hepatic lipid accumulation and fibrotic progression [43]. However, its safety and efficacy remain to be considered [44, 45]. The limited availability of therapeutic agents for MASLD stems from its complex pathophysiology, characterized by heterogeneous disease mechanisms involving both intrahepatic and systemic regulatory factors. Consequently, effective treatment strategies may necessitate pharmacological interventions with pleiotropic actions or synergistic combination therapies. However, SGLT2 inhibitors offer a unique advantage due to their pleiotropic effects on glucose homeostasis, lipid regulation, and fibrotic processes making them a promising therapeutic option for MASLD, particularly in patients with coexisting T2DM [46, 47].

This study has certain limitations that should be acknowledged. First, while SGLT2 inhibitors are reported to increase food intake in animal models, typically necessitating pair-feeding controls [48], we did not monitor food intake during the experiment, which may have influenced some results. Nevertheless, the observed improvements in liver mass, lipid profiles, and histology align with previous reports, supporting the reliability of our findings. Second, although our study comprehensively evaluated lipid accumulation, inflammation, oxidative

stress, and fibrosis, the molecular mechanisms require further exploration through in vitro studies.

In conclusion, our study demonstrates that dapagliflozin attenuates MASLD progression in DIO mice through multifaceted mechanisms, including the reduction of hepatic lipid accumulation, suppression of inflammatory responses, amelioration of oxidative stress, and inhibition of fibrotic processes. Notably, unlike previous studies that either failed to observe improvements in inflammation and systemic oxidative stress [19] or employed higher DaPa doses without significant effects on liver weight [18], our STZ/HFD-induced MASLD model with T2DM revealed comprehensive therapeutic effects at a commonly used dose, providing a more complete understanding of dapagliflozin's hepatoprotective potential. These findings not only highlight the therapeutic promise of SGLT2 inhibitors for MASLD management, particularly in patients with concurrent T2DM, but also underscore the importance of dose optimization and comprehensive metabolic evaluation in future investigations. While our preclinical results are encouraging, further clinical studies are warranted to validate these findings and explore the long-term benefits and safety profile of SGLT2 inhibitors in MASLD patients, potentially paving the way for novel therapeutic strategies in metabolic liver diseases.

Abbreviations

α	SMA Alpha-smooth muscle actin
ATF4	Activating transcription factor 4
CCL2	C-C motif chemokine ligand 2
cDNA	Complementary DNA
CHOP	C/EBP-homologous protein
CON	Control
CPT1 α	Carnitine Palmitoyltransferase 1 Alpha
CXCL1	C-X-C motif chemokine ligand 1
CXCL2	C-X-C motif chemokine ligand 2
DaPa	Dapagliflozin
DCFH-DA	2',7'-Dichlorodihydrofluorescein diacetate
DIO	Diet-induced obese
dUTP	Deoxyuridine triphosphate
F4/80	Epidermal growth factor-like module-containing mucin-like hormone receptor-like 1
GSH	Glutathione
HDL-C	High-density lipoprotein-cholesterol
H&E	Hematoxylin and eosin
HRP-DAB	Horseradish peroxidase-diaminobenzidine
HSCs	Hepatic stellate cells
IL-6	Interleukin-6
LDL-C	Low-density lipoprotein-cholesterol
MASLD	Metabolic dysfunction-associated steatotic liver disease
MDA	Malondialdehyde
MPO	Myeloperoxidase
NLRP3 NOD	LRR- and Pysin Domain-Containing Protein 3
PGC1- α	Peroxisome Proliferator-Activated Receptor Gamma Coactivator 1-Alpha
PPAR α	Peroxisome Proliferator-Activated Receptor Alpha
Ptgs2	Prostaglandin-endoperoxide synthase 2
qRT-PCR	Quantitative real-time polymerase chain reaction
ROS	Reactive oxygen species;
SGLT2	Sodium-glucose cotransporter-2
STZ	Streptozotocin
TC	Total cholesterol

T2DM	Type 2 diabetes mellitus
TG	Triglyceride
THR- β	Thyroid hormone receptor beta
TNF- α	Tumor necrosis factor-alpha
TUNEL	Terminal deoxynucleotidyl transferase dUTP nick-end labeling
XBP1	X-box binding protein 1

Supplementary Information

The online version contains supplementary material available at <https://doi.org/10.1186/s40360-025-00898-z>.

Supplementary Material 1

Acknowledgements

We acknowledge the experimental platform provided by the Scientific Research and Experiment Center of the Second Affiliated Hospital of Anhui Medical University.

Author contributions

T.P., X.Z., Y.W., designed research; X.F., Y.W. and H.D. performed research; X.F., Y.W., Y.Y.W., Y.D. and X.Z. analyzed data; X.F., Y.W., X.Z., and T.P. wrote the manuscript. All authors read and approved the final manuscript.

Funding

This work was supported by National Natural Science Foundation of China (82200805), the Key Project of Natural Science Research of Anhui Higher Education Institution (2023AH053182), Health Research Program of Anhui (AHWJ2023A10010, AHWJ2023BAC10010, AHWJ2023BAC10016).

Data availability

No datasets were generated or analysed during the current study.

Declarations

Ethics approval and consent to participate

All animal experiments were approved by the Animal Experimental and Ethics Committee of the Second Affiliated Hospital of Anhui Medical University and performed in compliance with the guidelines of the Committee of Animal Care and Use of the Second Affiliated Hospital of Anhui Medical University and ARRIVE guidelines.

Consent for publication

Not applicable.

Competing interests

The authors declare no competing interests.

Received: 15 December 2024 / Accepted: 7 March 2025

Published online: 12 March 2025

References

1. Younossi ZM, Golabi P, Paik JM, Henry A, Van Dongen C, Henry L. The global epidemiology of nonalcoholic fatty liver disease (NAFLD) and nonalcoholic steatohepatitis (NASH): a systematic review. *Hepatology* (Baltimore MD). 2023;77:1335–47. <https://doi.org/10.1097/hep.0000000000000004>.
2. Monsénégó J, Mansouri A, Akkaoui M, Lenoir V, Esnous C, Fauveau V, Tavernier V, Girard J, Prip-Buus C. Enhancing liver mitochondrial fatty acid oxidation capacity in obese mice improves insulin sensitivity independently of hepatic steatosis. *J Hepatol*. 2012;56:632–9. <https://doi.org/10.1016/j.jhep.2011.10.008>.
3. Sheka AC, Adeyi O, Thompson J, Hameed B, Crawford PA, Ikramuddin S. Nonalcoholic steatohepatitis: A review. *JAMA*. 2020;323:1175–83. <https://doi.org/10.1001/jama.2020.2298>.
4. Peverill W, Powell LW, Skoien R. Evolving concepts in the pathogenesis of NASH: beyond steatosis and inflammation. *Int J Mol Sci*. 2014;15:8591–638. <https://doi.org/10.3390/ijms15058591>.

5. Rinella ME, Neuschwander-Tetri BA, Siddiqui MS, Abdelmalek MF, Caldwell S, Barb D, Kleiner DE, Loomba R. AASLD practice guidance on the clinical assessment and management of nonalcoholic fatty liver disease. *Hepatology* (Baltimore MD). 2023;77:1797–835. <https://doi.org/10.1097/hep.0000000000000323>.
6. Rinella ME, Lazarus JV, Ratzliff V, Francque SM, Sanyal AJ, Kanwal F, Romero D, Abdelmalek MF, Anstee QM, Arab JP, et al. A multisociety Delphi consensus statement on new fatty liver disease nomenclature. *Ann Hepatol*. 2024;29:101133. <https://doi.org/10.1016/j.aohep.2023.101133>.
7. Wang M, Zhao Y, He Y, Zhang L, Liu J, Zheng S, Bai Y. The bidirectional relationship between NAFLD and type 2 diabetes: A prospective population-based cohort study. *Nutrition, metabolism, and cardiovascular diseases. NMCD*. 2023;33:1521–8. <https://doi.org/10.1016/j.numecd.2023.05.018>.
8. Mantovani A, Petracca G, Beatrice G, Tilg H, Byrne CD, Targher G. Non-alcoholic fatty liver disease and risk of incident diabetes mellitus: an updated meta-analysis of 501 022 adult individuals. *Gut*. 2021;70:962–9. <https://doi.org/10.1136/gutjnl-2020-322572>.
9. Tilg H, Moschen AR, Roden M. NAFLD and diabetes mellitus. *Nat Rev Gastroenterol Hepatol*. 2017;14:32–42. <https://doi.org/10.1038/nrgastro.2016.147>.
10. Choi DH, Jung CH, Mok JO, Kim CH, Kang SK, Kim BY. Effect of Dapagliflozin on Alanine aminotransferase improvement in type 2 diabetes mellitus with Non-alcoholic fatty liver disease. (Seoul Korea). 2018;33:387–94. <https://doi.org/10.3803/EnM.2018.33.3.387>. Endocrinology and metabolism.
11. Gastaldelli A, Repetto E, Guja C, Hardy E, Han J, Jabbar SA, Ferrannini E. Exenatide and Dapagliflozin combination improves markers of liver steatosis and fibrosis in patients with type 2 diabetes. *Diabetes Obes Metab*. 2020;22:393–403. <https://doi.org/10.1111/dom.13907>.
12. Shimano H. Sterol regulatory element-binding protein-1 as a dominant transcription factor for gene regulation of lipogenic enzymes in the liver. *Trends Cardiovasc Med*. 2000;10:275–8. [https://doi.org/10.1016/s1050-1738\(00\)00079-7](https://doi.org/10.1016/s1050-1738(00)00079-7).
13. Shimizu M, Suzuki K, Kato K, Jojima T, Iijima T, Murohisa T, Iijima M, Takekawa H, Usui I, Hiraishi H, et al. Evaluation of the effects of Dapagliflozin, a sodium-glucose co-transporter-2 inhibitor, on hepatic steatosis and fibrosis using transient elastography in patients with type 2 diabetes and non-alcoholic fatty liver disease. *Diabetes Obes Metab*. 2019;21:285–92. <https://doi.org/10.1111/dom.13520>.
14. Latva-Rasku A, Honka MJ, Kullberg J, Mononen N, Lehtimäki T, Saltevo J, Kirjavainen AK, Saunavaara V, Iozzo P, Johansson L, et al. The SGLT2 inhibitor Dapagliflozin reduces liver fat but does not affect tissue insulin sensitivity: A randomized, Double-Blind, Placebo-Controlled study with 8-Week treatment in type 2 diabetes patients. *Diabetes Care*. 2019;42:931–7. <https://doi.org/10.2337/dc18-1569>.
15. Scheen AJ. Beneficial effects of SGLT2 inhibitors on fatty liver in type 2 diabetes: A common comorbidity associated with severe complications. *Diabetes Metab*. 2019;45:213–23. <https://doi.org/10.1016/j.diabet.2019.01.008>.
16. Harrison SA, Manghi FP, Smith WB, Alpeidze D, Aizenberg D, Klarenbeek N, Chen CY, Zuckerman E, Ravussin E, Charatcharoenwithaya P, et al. Licoglitazone for nonalcoholic steatohepatitis: a randomized, double-blind, placebo-controlled, phase 2a study. *Nat Med*. 2022;28:1432–8. <https://doi.org/10.1038/s41591-022-01861-9>.
17. Hiruma S, Shigiyama F, Kumashiro N. Empagliflozin versus sitagliptin for ameliorating intrahepatic lipid content and tissue-specific insulin sensitivity in patients with early-stage type 2 diabetes with non-alcoholic fatty liver disease: A prospective randomized study. *Diabetes Obes Metab*. 2023;25:1576–88. <https://doi.org/10.1111/dom.15006>.
18. Luo J, Sun P, Wang Y, Chen Y, Niu Y, Ding Y, Xu N, Zhang Y, Xie W. Dapagliflozin attenuates steatosis in livers of high-fat diet-induced mice and oleic acid-treated L02 cells via regulating AMPK/mTOR pathway. *Eur J Pharmacol*. 2021;907:174304. <https://doi.org/10.1016/j.ejphar.2021.174304>.
19. Han T, Fan Y, Gao J, Fatima M, Zhang Y, Ding Y, Bai L, Wang C. Sodium glucose cotransporter 2 inhibitor Dapagliflozin depressed adiposity and ameliorated hepatic steatosis in high-fat diet induced obese mice. *Adipocyte*. 2021;10:446–55. <https://doi.org/10.1080/21623945.2021.1979277>.
20. Xiang L, Liu M, Xiang G, Yue L, Zhang J, Xu X, Dong J. Dapagliflozin promotes white adipose tissue Browning through regulating angiogenesis in high fat induced obese mice. *BMC Pharmacol Toxicol*. 2024;25:26. <https://doi.org/10.1186/s40360-024-00747-5>.
21. Binch A, Snuggs J, Le Maitre CL. Immunohistochemical analysis of protein expression in formalin fixed paraffin embedded human intervertebral disc tissues. *JOR Spine*. 2020;3:e1098. <https://doi.org/10.1002/jsp2.1098>.
22. Riazi K, Azhari H, Charette JH, Underwood FE, King JA, Afshar EE, Swain MG, Congly SE, Kaplan GG, Shaheen AA. The prevalence and incidence of NAFLD worldwide: a systematic review and meta-analysis. *Lancet Gastroenterol Hepatol*. 2022;7:851–61. [https://doi.org/10.1016/s2468-1253\(22\)00165-0](https://doi.org/10.1016/s2468-1253(22)00165-0).
23. Amangurbanova M, Huang DQ, Noureddin N, Tesfai K, Bettencourt R, Siddiqi H, Lopez SJ, Cervantes V, Madamba E, Loomba R. A prospective study on the prevalence of MASLD in patients with type 2 diabetes and hyperferritinemia. *Aliment Pharmacol Ther*. 2025;61:456–64. <https://doi.org/10.1111/apt.18377>.
24. Deng M, Wen Y, Yan J, Fan Y, Wang Z, Zhang R, Ren L, Ba Y, Wang H, Lu Q, et al. Comparative effectiveness of multiple different treatment regimens for nonalcoholic fatty liver disease with type 2 diabetes mellitus: a systematic review and bayesian network meta-analysis of randomised controlled trials. *BMC Med*. 2023;21:447. <https://doi.org/10.1186/s12916-023-03129-6>.
25. Lee JY, An M, Heo H, Park JY, Lee J, Kang CH. *Limosilactobacillus fermentum* MG4294 and *Lactiplantibacillus plantarum* MG5289 ameliorates nonalcoholic fatty liver disease in High-Fat Diet-Induced mice. *Nutrients*. 2023;15. <https://doi.org/10.3390/nu15082005>.
26. Rakhshandehroo M, Hooiveld G, Müller M, Kersten S. Comparative analysis of gene regulation by the transcription factor PPARalpha between mouse and human. *PLoS ONE*. 2009;4:e6796. <https://doi.org/10.1371/journal.pone.0006796>.
27. Androutsakos T, Nasiri-Ansari N, Bakasis AD, Kyrou I, Efstathiopoulos E, Randevas HS, Kassi E. SGLT-2 inhibitors in NAFLD: expanding their role beyond diabetes and cardioprotection. *Int J Mol Sci*. 2022;23. <https://doi.org/10.3390/ijms23063107>.
28. Peiseler M, Schwabe R, Hampe J, Kubes P, Heikenwälder M, Tacke F. Immune mechanisms linking metabolic injury to inflammation and fibrosis in fatty liver disease - novel insights into cellular communication circuits. *J Hepatol*. 2022;77:1136–60. <https://doi.org/10.1016/j.jhep.2022.06.012>.
29. Duan Y, Pan X, Luo J, Xiao X, Li J, Bestman PL, Luo M. Association of inflammatory cytokines with Non-Alcoholic fatty liver disease. *Front Immunol*. 2022;13:880298. <https://doi.org/10.3389/fimmu.2022.880298>.
30. Sayour AA, Korkmaz-Icöz S, Loganathan S, Ruppert M, Sayour VN, Oláh A, Benke K, Brune M, Benkő R, Horváth EM, et al. Acute Canagliflozin treatment protects against in vivo myocardial ischemia-reperfusion injury in non-diabetic male rats and enhances endothelium-dependent vasorelaxation. *J Translational Med*. 2019;17:127. <https://doi.org/10.1186/s12967-019-1881-8>.
31. Tahara A, Kurosaki E, Yokono M, Yamajuku D, Kihara R, Hayashizaki Y, Takasu T, Imamura M, Li Q, Tomiyama H, et al. Effects of SGLT2 selective inhibitor Ipragliflozin on hyperglycemia, hyperlipidemia, hepatic steatosis, oxidative stress, inflammation, and obesity in type 2 diabetic mice. *Eur J Pharmacol*. 2013;715:246–55. <https://doi.org/10.1016/j.ejphar.2013.05.014>.
32. Zhang R, Xie Q, Lu X, Fan R, Tong N. Research advances in the anti-inflammatory effects of SGLT inhibitors in type 2 diabetes mellitus. *Diabetol Metab Syndr*. 2024;16:99. <https://doi.org/10.1186/s13098-024-01325-9>.
33. Luci C, Bourinet M, Leclère PS, Anty R, Gual P. Chronic inflammation in Non-Alcoholic steatohepatitis: molecular mechanisms and therapeutic strategies. *Front Endocrinol*. 2020;11:597648. <https://doi.org/10.3389/fendo.2020.597648>.
34. Gensluckner S, Wernly B, Datz C, Aigner E. Iron, oxidative stress, and metabolic Dysfunction-Associated steatotic liver disease. *Antioxid (Basel Switzerland)*. 2024;13. <https://doi.org/10.3390/antiox13020208>.
35. Pruetz JE, Everman SJ, Hoang NH, Salau F, Taylor LC, Edwards KS, Hosler JP, Huffman AM, Romero DG, Yanes Cardozo LL. Mitochondrial function and oxidative stress in white adipose tissue in a rat model of PCOS: effect of SGLT2 Inhibition. *Biology Sex Differences*. 2022;13(45). <https://doi.org/10.1186/s13293-022-00455-x>.
36. Luna-Marco C, Iannantuoni F, Hermo-Argibay A, Devos D, Salazar JD, Víctor VM, Rovira-Llopis S. Cardiovascular benefits of SGLT2 inhibitors and GLP-1 receptor agonists through effects on mitochondrial function and oxidative stress. *Free Radic Biol Med*. 2024;213:19–35. <https://doi.org/10.1016/j.freeradbiomed.2024.01.015>.
37. Leng W, Wu M, Pan H, Lei X, Chen L, Wu Q, Ouyang X, Liang Z. The SGLT2 inhibitor Dapagliflozin attenuates the activity of ROS-NLRP3 inflammasome axis in steatohepatitis with diabetes mellitus. *Annals Translational Med*. 2019;7:429. <https://doi.org/10.21037/atm.2019.09.03>.
38. Lee KC, Wu PS, Lin HC. Pathogenesis and treatment of non-alcoholic steatohepatitis and its fibrosis. *Clin Mol Hepatol*. 2023;29:77–98. <https://doi.org/10.3350/cmh.2022.0237>.

39. Tsuchida T, Friedman SL. Mechanisms of hepatic stellate cell activation. *Nat Rev Gastroenterol Hepatol*. 2017;14:397–411. <https://doi.org/10.1038/nrgastro.2017.38>.
40. Heo YJ, Lee N, Choi SE, Jeon JY, Han SJ, Kim DJ, Kang Y, Lee KW, Kim HJ. Empagliflozin reduces the progression of hepatic fibrosis in a mouse model and inhibits the activation of hepatic stellate cells via the Hippo signalling pathway. *Biomedicines*. 2022;10. <https://doi.org/10.3390/biomedicines10051032>.
41. Shen Y, Cheng L, Xu M, Wang W, Wan Z, Xiong H, Guo W, Cai M, Xu F. SGLT2 inhibitor empagliflozin downregulates miRNA-34a-5p and targets GREM2 to inactivate hepatic stellate cells and ameliorate non-alcoholic fatty liver disease-associated fibrosis. *Metab Clin Exp*. 2023;146:155657. <https://doi.org/10.1016/j.metabol.2023.155657>.
42. Zhou P, Tan Y, Hao Z, Xu W, Zhou X, Yu J. Effects of SGLT2 inhibitors on hepatic fibrosis and steatosis: A systematic review and meta-analysis. *Front Endocrinol*. 2023;14:1144838. <https://doi.org/10.3389/fendo.2023.1144838>.
43. Kokkorakis M, Boutari C, Hill MA, Kotsis V, Loomba R, Sanyal AJ, Mantzoros CS. Resmetirom, the first approved drug for the management of metabolic dysfunction-associated steatohepatitis: trials, opportunities, and challenges. *Metab Clin Exp*. 2024;154:155835. <https://doi.org/10.1016/j.metabol.2024.155835>.
44. H. The Lancet Gastroenterology. Resmetirom for NASH: balancing promise and Prudence. *The Lancet. Gastroenterol Hepatol*. 2024;9:273. [https://doi.org/10.1016/s2468-1253\(24\)00049-9](https://doi.org/10.1016/s2468-1253(24)00049-9).
45. Cusi K. Selective agonists of thyroid hormone receptor Beta for the treatment of NASH. *N Engl J Med*. 2024;390:559–61. <https://doi.org/10.1056/NEJMe2314365>.
46. Mantovani A, Petracca G, Csermely A, Beatrice G, Targher G. Sodium-Glucose Cotransporter-2 inhibitors for treatment of nonalcoholic fatty liver disease: A Meta-Analysis of randomized controlled trials. *Metabolites*. 2020;11. <https://doi.org/10.3390/metabo11010022>.
47. Arai T, Atsukawa M, Tsubota A, Mikami S, Haruki U, Yoshikata K, Ono H, Kawano T, Yoshida Y, Tanabe T, et al. Antifibrotic effect and long-term outcome of SGLT2 inhibitors in patients with NAFLD complicated by diabetes mellitus. *Hepatol Commun*. 2022;6:3073–82. <https://doi.org/10.1002/hep4.2069>.
48. Masuda T, Watanabe Y, Fukuda K, Watanabe M, Onishi A, Ohara K, Imai T, Koepsell H, Muto S, Vallon V, et al. Unmasking a sustained negative effect of SGLT2 Inhibition on body fluid volume in the rat. *American journal of physiology. Ren Physiol*. 2018;315:F653–64. <https://doi.org/10.1152/ajprenal.00143.2018>.

Publisher's note

Springer Nature remains neutral with regard to jurisdictional claims in published maps and institutional affiliations.